Experimental and theoretical insights on the thermal oxidation of epoxy-amine networks

Romain Delannoy, Vincent Tognetti, Emmanuel Richaud

Experimental and theoretical insights on the thermal oxidation of epoxy-amine networks

Romain Delannoy [a,b], Vincent Tognetti [b], Emmanuel Richaud [a,*]

[a] Laboratoire PIMM, Arts et Metiers Institute of Technology, CNRS Cnam, HESAM Universite, 151 boulevard de l'Hopital, Paris 75013, France
[b] COBRA UMR 6014 & FR 3038, Normandy University, Université de Rouen, INSA Rouen, CNRS, 1 rue Tesniere, Mont St Aignan 76821 CEDEX, France

ARTICLE INFO

Keywords:
Epoxy-amine
Thermal oxidation
Machine learning
Bond dissociation energy
Propagation step

ABSTRACT

This paper reports an investigation of the oxidation of three epoxy-amine networks obtained from DGEBA cured with three sorts of aliphatic hardeners ethylene diamine (EDA), diethylene triamine (DETA), and triethylene tetraamine (TETA). Oxidation was monitored by FTIR with an innovative discussion of CH_2 consumption. Methylene groups held by hardeners groups were shown to be more sensitive to oxidation, which was confirmed by a discussion of Bond Dissociation Energies (BDE) computed by a machine-learning approach.

1. Introduction

Epoxies are increasingly used in industrial applications with strong requirements in terms of durability such as the design of lightened composite parts for engines in aeronautic field or waterproofing of concrete substrates in civil engineering [1]. The lack of feedback on such materials together with the complexity of ageing conditions (and the difficulty to correlate them) with an accelerated ageing test makes necessary to predict their lifetime by a non-empirical approach based on the determination of ageing rates.

Epoxy ageing is already well documented in literature. It is known they can undergo a (reversible) physical ageing by water permeation [2–4] and/or structural relaxation [5], or (irreversible) chemical ageing by radio-oxidation, photo-oxidation, or thermal oxidation [6–9]. In any case, but more generally for oxidative ageing, the prediction of lifetime is based on the use of a kinetic model. Such models are easily implemented with a thorough knowledge of the chemical reactions involved in degradation. For example, complete modelling describing the reactivity of tertiary C–H groups has been proposed to study the degradation of polypropylene [10], and more complex kinetic models describing the reactivity of allylic C–H groups were proposed for polyisoprene [11] and polychloroprene [12].

The level of difficulty increases when it comes to understanding the ageing of epoxy-amine networks. The wide variety of epoxide prepolymers and hardeners that they are made of allows for an almost infinite number of mixtures differing by their viscosity, reactivity, and final properties, to suit and meet industrial requirements. Even in the simplest epoxy-diamine binary mixtures, the complex molecular structure presents many possible reactive groups, making the implementation of a representative kinetic model more intricate.

Previous works have already discussed on the nature of stable carbonyl products formed during oxidation to distinguish the nature of reactive sites involved in their formation [13]. However, several difficulties arise mainly due to the complex overlap of FTIR signals attributed to stable products in a relatively narrow wavenumber range, combined with the speculative aspect of radical mechanism in solid structures [14].

The aim of the present study is to illustrate a possible solution to identify reactive sites in epoxy-amine networks by using the combination of two complementary tools:

- An identification of reactive groups based on a thorough analysis of C–H stretching wavenumber range in FTIR.
- A discussion on the Bond Dissociation Energies of reactive groups (as bonds weaknesses may be the "driving force" of radical oxidation) with a theoretical approach based on a convenient machine-learning tool, which will first be validated by computational QC (quantum chemistry) calculations.

2. Materials and methods

2.1. Epoxy-amine thermoset materials

Epoxy-amine systems were prepared by blending DGEBA (D.E.R. 332, CAS 1675-54-35 supplied by Sigma Aldrich, epoxide equivalent weight EEW 171-175 g/eq) with one of three aliphatic amine hardeners: ethylene diamine EDA (CAS 107-15-3, Sigma Aldrich, amine hardener equivalent weight AHEW 15.0 g/eq), diethylene triamine DETA (CAS 11-40-0, Sigma Aldrich, AHEW 20.6 g/eq), or triethylene tetraamine TETA (CAS 112-24-3, Sigma Aldrich, AHEW 24.4 g/eq) (Fig. 1). The two components were mixed in stoichiometric proportions to obtain ideal networks with a well-defined chemical structure. The three networks will further be called DGEBA-EDA, DGEBA-DETA, and DGEBA-TETA.

After mixing, the blends were set to thicken for up to 3 h in closed vials to avoid hardener evaporation. Thermoset films – of thickness 20–60 µm (measured with a manual micrometre) with an experimental uncertainty of 5 µm – were then manufactured using a heating hydro-press (Gibitre), and cured for 1 h at 50 °C, followed by 1 h at 90 °C. Post-curing for 30 min at 170 °C under vacuum was finally carried out to ensure complete curing of the networks (by heating over the expected glass transition of the polymer). This protocol was followed very rigorously to acquire near-ideal molecular structure of the networks. Its reliability was checked by a comparison of the glass transition values with those coming from the prediction method given by Bellenger et al. [15] (**see Suppl. Info. 1**).

Differential scanning calorimetry (DSC) was performed at 10 °C min^{-1} – using a DSC Q10 provided by TA Instruments – to confirm the absence of any residual exothermic curing peak and to characterize the glass transition of unaged samples (Fig. 2). Glass transition temperatures of unaged samples were identified on the second heating ramp at 143 °C, 147 °C, and 149 °C for DGEBA-EDA, DGEBA-DETA, and DGEBA-TETA, respectively. FTIR measurements were also carried out to confirm the disappearance of epoxides – with characteristic peak [16] at 915 cm^{-1} – and the absence of oxidation of the unaged samples – with characteristic peaks between 1650 and 1800 cm^{-1}.

2.2. Thermal ageing protocol

To understand their influence on oxidizability, several temperature conditions were studied. As such, networks were aged at 80, 100, 120, 140 and 160 °C under air in ventilated ovens. Samples were then periodically removed for FTIR measurements. Since glass transition of networks under investigation are very close (about 145 °C), those ageing temperatures were selected so as to compare their ageing either in glassy or rubbery state.

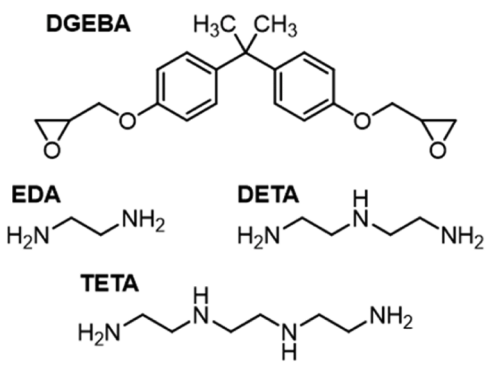

Fig. 1. Chemical formulas of monomers used for the formation of epoxy-amine networks.

2.3. Experimental measurements

FTIR spectroscopy in transmission mode was carried out using a Frontier spectrophotometer (PerkinElmer) by averaging 8 scans at resolution 4 cm^{-1} between 400 and 4000 cm^{-1}. Absorbances were measured by subtracting baseline and defined as the maximum height of characteristic peaks, on up to 3 samples to check for repeatability of measurements. Beer-Lambert law was used to calculate concentrations of amide groups, with molar attenuation coefficient [14] for its characteristic peak at 1660 cm^{-1} of 400 L mol^{-1} cm^{-1}. As determining an accurate coefficient is rather challenging, this approximate value was chosen to maximize the calculated concentrations for an estimation of the oxidation process advancement. As a common coefficient is used for the three epoxy-amine networks, a different value does not change the observations drawn in this paper.

3. Results

3.1. Appearance of oxidized products

Formation of oxidized groups were followed by FTIR, and spectra of the three epoxy-amine systems aged at 120 °C in the 1625–1800 cm^{-1} wavenumber range are stacked in Fig. 3. Significant increases in absorbance can be identified during the ageing with maxima around 1660 cm^{-1} and 1740 cm^{-1}, respectively attributed to the formation of amide and other carbonyl groups [14]. The latter is assumed to stem from one of various C=O bonds species such as imides, carboxylic acids and esters [13,17], but will not be further discussed here as it is not the main product of this particular oxidation. A small shift is observed for the amide group compared to our previous observations [13], possibly due to electronic effects induced by $–SO_2$-Ar- groups.

As the molecular structure of the oxidized polymer is expected to present a blend of oxidized functions with different chemical environments, it is rather difficult to assess an accurate molar attenuation coefficient for each function [14]. Nonetheless, assuming the chosen coefficient values are acceptable to estimate the concentrations, it appears that amide groups are the main products of the thermal oxidation. Amide concentrations for the three systems at 120 °C under air are plotted over ageing time in Fig. 4. The Gaussian deconvolutions of the spectral region ranging from 1600 to 1800 cm^{-1} for these spectra show no apparent overlapping of the two peaks (at 1660 and 1740 cm^{-1}) that may alter the maxima values **[see Suppl. Info. 2]**. Let us precise that the peak centred at 1740 cm^{-1} was not deconvoluted anymore.

Curves at all temperatures exhibit a sigmoidal shape (less obvious at higher temperatures). First there is a slight induction period, then the auto-accelerated oxidation occurs. Lastly a noticeable plateau can be observed during which the amide groups production – or to be more exact, the appearance of its characteristic FTIR peak – appears to be slowed down.

The exact origin of this plateau remains unknown and open to interpretations as the oxidation mechanism in polymers is complex and implies many competing phenomena that may affect measurements. At first, as it will be developed in the following part, the consumption of oxidizable site will slow down the oxidation. The formation of this plateau may also be induced not only by the formation of low-mass volatile compounds [18], but also as imide groups are accumulated within the network, as its bands overlap with those of amide groups [13].

Although they present slight differences in molecular structure (with the presence of secondary N–H bonds in DETA and TETA hardeners), one can observe that DGEBA TETA oxidizes slightly faster than DGEBA-DETA, itself slightly faster than DGEBA-EDA (see also **Supp. Info. 5**). This will be discussed in the following in terms of concentration in reactive sites.

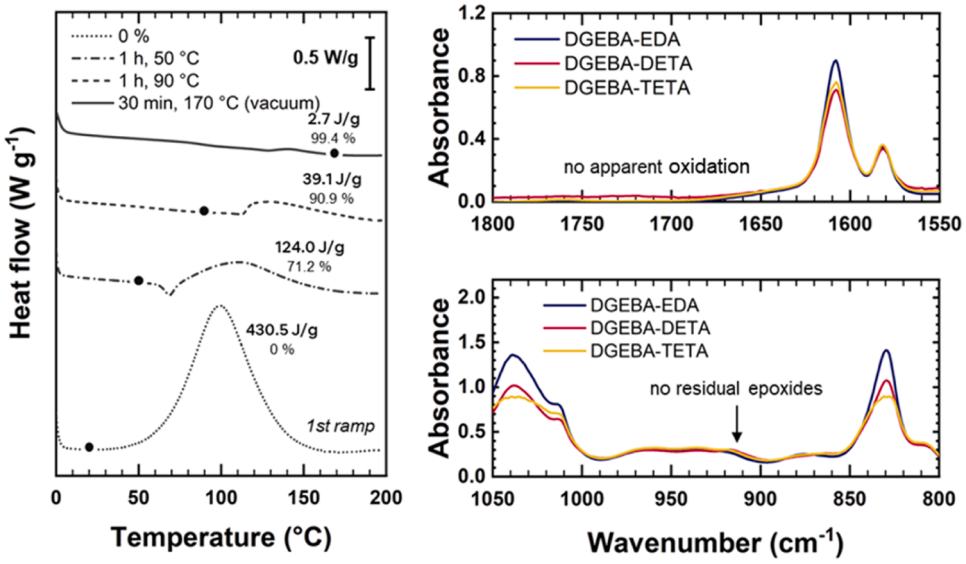

Fig. 2. Curing process analysis. (left) DSC ramps at 10 °C min^{-1} after each step show the disappearance of an exothermic curing peak – (right) FTIR spectra of unaged samples.

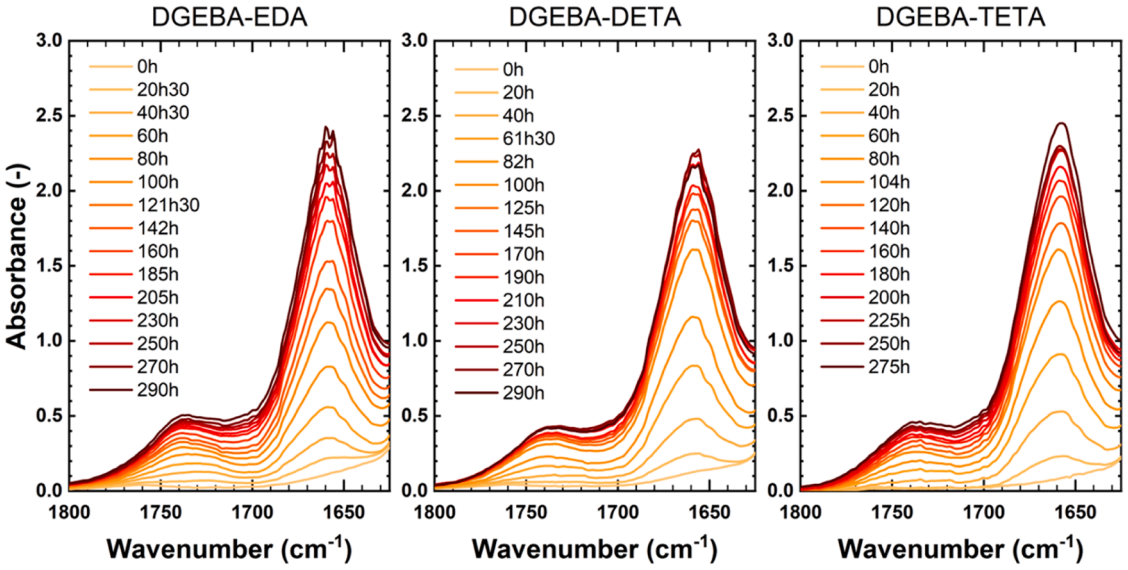

Fig. 3. FTIR spectra of the carbonyl region during the thermal oxidation of epoxy-amine samples at 120°C. Thickness were normalized at 30 µm.

3.2. C-H bonds disappearance during oxidation

The wavenumber range between 2750 and 3000 cm^{-1} was also studied to follow the changes in C–H bonds during the thermal ageing. FTIR spectra for aged networks at 120 °C are stacked in Fig. 5. Several maxima at 2830 cm^{-1}, 2872 cm^{-1}, 2933 cm^{-1} and 2966 cm^{-1}, and two small shoulders around 2890 cm^{-1} and 2910 cm^{-1} are observed. As it is rather difficult to properly allocate each peak in such a small wavenumber range, a proposition for their general assignment [19] is given in Table 1. A discussion on peak allocation by comparison with other DGEBA-amine networks presenting various hardener molecular structures (linear, aromatic, aliphatic cyclic, etc.) be found in **S.I.** In the following, it will be considered that 2830 cm^{-1} corresponds to "hardener" methylene. Interestingly, the ratio of absorbances at 2830 to 2966 one (methyl of DGEBA group) increases in line with the relative concentrations $[N\text{-}CH_2]_{hardener}/[\text{-}CH_3]_{DGEBA}$ in the three system under investigation.

A global decrease of convoluted peaks can be seen during the thermal oxidation, with one peak at 2830 cm^{-1} that appears to drastically reduce, suggesting the disappearance of one specific C–H function. Peaks were deconvoluted, using a 4-peak deconvolution method (two tentative 6-peak deconvolution methods are given in S.I. Section 4), for a better understanding of the changes in C–H bonds throughout the thermal oxidation. Deconvoluted curves are presented in Fig. 5 and were obtained in two steps: linear baseline correction followed by data fitting of the gaussian peaks sum with a Python script (mainly using SciPy library for the fit optimization) (S.I. section 4). Following tentative assignment of the peaks [19], several conclusions can be drawn:

- Isopropyl CH_3 groups located between aromatic rings of DGEBA appear to be stable to the thermal oxidation of the network as peaks at 2966 cm^{-1} and 2872 cm^{-1} barely decrease with ageing.
- The three types of CH_2 groups next to a heteroatom (N or O) can hardly be differentiated within the peak at 2933 cm^{-1}, which appears to decrease but not to the same degree as the peak at 2830 cm^{-1}.

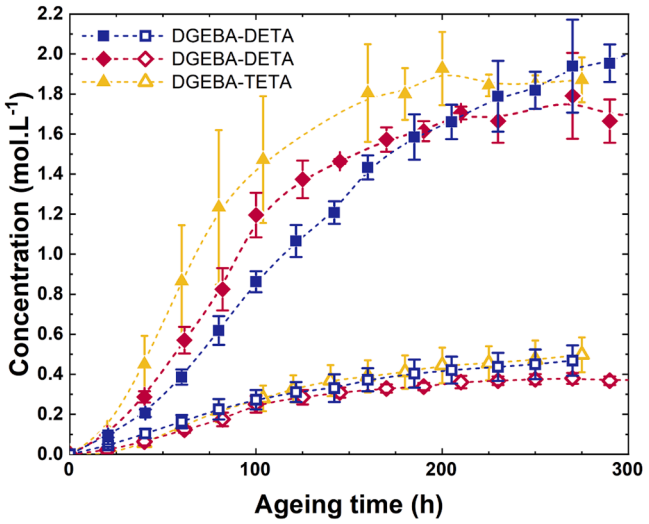

Fig. 4. Changes in amide groups concentrations at 120 °C under air. Open symbols represent carbonyls with FTIR signal around 1730 cm^{-1} (using $\varepsilon = 300$ l mol^{-1} cm^{-1}) and closed symbols amides at 1660 cm^{-1}.

N–CH_2–CH_2 groups located on the hardener side, with characteristic peak at 2830 cm^{-1}, mostly disappear with the oxidation of the network, suggesting they are responsible for the formation of oxidized products. As the deconvolution spectra show that the 2830 cm^{-1} peak maxima barely overlap with neighbouring peaks, the method was considered satisfactory for detecting consumption of hardener CH_2 during ageing.

Although the peak at 2830 cm^{-1} clearly disappears with ageing, and according to the spectra presented in Fig. 6, it is unclear if both amine-yielding methylene groups located either within the "epoxy" or "hardener" moiety really take part in the oxidation process. In fact, since the oxidation of one methylene seems to induce some changes in the FTIR absorbance of the other -CH_2- connected to the same nitrogen atom, it is possible that the observed 80% decrease of 2830 cm^{-1} absorbance corresponds to a lower ratio of consumed >N-CH_2.

4. Discussion

The main goal of this section is to understand the differences in reactivity of all the oxidizable sites within the molecular structure of systems under study. As such, we will:

- Validate a method to easily assess the bond dissociation energies (BDE) of epoxy-amine networks under study by comparing results from composite QC method and easy-to-use machine-learning model for small representative molecules.
- Apply this machine-learning approach for the description of all C–H bonds of interest in molecules representative of the constitutive repetitive units.
- Discuss on the fate of those C–H bonds in terms of degradation mechanisms and more particularly on stable products, to assess the representativeness of accelerated ageing and later the possibility to extrapolate data to low temperature ageing. As systems under study have almost the same glass transition temperature, that possible difference only comes from an intrinsic difference in reactivity and are not due to a "mobility-reactivity" coupling. Eventually, evidence of the major reactivity of one kind of C-H compared to others would allow to conclude about the "unicity" of a propagation process ROO° + RH → ROOH + R°. A simpler kinetic model based on the reactivity of only one reactive site (RH) could then be considered, where rate constants depict the reality of reactive species (R°, ROO°, ROOH…) identically for example to the case of polyethylene [20].

4.1. On the use of machine learning approach for BDE calculations

A recent computational tool will be validated and used to tackle this crucial physicochemical feature. To this aim, St John *et al*'s machine learning (ML) model, which only requires the SMILES code of the molecule, was assessed specifically for the prediction of C-H standard dissociation enthalpies on secondary and tertiary carbon atoms using the accurate CBS-QB3 [21] composite method (considered here as reference) that includes a full density functional theory (DFT) 3D-optimization of the molecular geometry followed by subsequent post-Hartree-Fock energy calculations (up to the CCSD(T) level with complete basis set extrapolation), which provides the so-called "chemical accuracy" (absolute error lower than 1 kcal mol^{-1} in average) for atomization enthalpies. All QC calculations were performed with the Gaussian 09 package [22].

For this purpose, a representative dataset of 25 molecules with secondary carbon atoms was first considered, gathering the main chemical functions involving carbon, nitrogen, and oxygen atoms. The datasets are further described in the **Suppl. Info. 5 file**. It collects, in a balanced way, alkanes, alkenes, ethers, alcohols, aldehydes and ketones, carboxylic acids, esters, amines, amides, nitriles and imines, which were also chosen so that they do not exhibit conformational complexity. The $\Delta H°_{dissoc}^{CBS-QB3}$ values span a large range (about 60 kJ mol^{-1}, 16% of the average value), between 346.9 and 407.5 kJ mol^{-1} with a mean value equal to 379.6 kJ mol^{-1}, proving evidence that the C-H bond strength in CH_2 group can be considerably influenced by its substituents.

Similarly, a set of 15 molecules featuring a tertiary carbon atom was considered. The range for $\Delta H°_{dissoc}^{CBS-QB3}$ values is close to that for secondary cases (from 351.7 to 417.3 kJ mol^{-1}, with an average value equal to 383.5 kJ mol^{-1}). This suggests that secondary and tertiary C-H can be both prone to dissociation, and that one cannot determine the preferential oxidation site only based on the intrinsic carbon class.

These results also give evidence that the ML model systematically underestimates $\Delta H°_{dissoc}$, the mean signed deviation (MSD) with respect to CBS-QB3 being equal to -6.1 kJ mol^{-1} for secondary carbons and -9.4 kJ mol^{-1} for tertiary ones. This hints that the ML model, which was not specifically trained for such bonds, can be however considered a suitable departure point for the studied issue. Noteworthy, the ML and CBS-QB3 enthalpy series are strongly linearly correlated ($R^2 = 0.98$ for secondary group and 0.99 for tertiary subset, see Fig. 7), according to:

$$\Delta H°_{dissoc}^{model} = -45.7 + 1.14\Delta H°_{dissoc}^{ML}\big|_{kJ\ mol^{-1}} \ (secondary) \quad (1a)$$

$$\Delta H°_{dissoc}^{model} = -13.6 + 1.06\Delta H°_{dissoc}^{ML}\big|_{kJ\ mol^{-1}} \ (tertiary) \quad (1b)$$

These models afford a significant improvement since the corresponding MAD value is equal to 1.7 (secondary) and 1.3 kJ mol^{-1} (tertiary). In conclusion, these corrected ML models provide a reliable and very fast prediction of $\Delta H°_{dissoc}$, equivalent to CBS-QB3, but at negligible computational cost.

4.2. On the oxidizability of networks under study

The models were then applied to the molecules of interest, as depicted later in Fig. 9. These molecules were chosen as they replicate the constitutive repetitive units of the network except for methyl groups on the outer branching to the next unit. It should be noted that these molecules can also be obtained following the reaction between 1,2-epoxy-3-phenoxypropane EPP and the studied hardeners, and will be further called EPP-EDA, EPP-DETA, and EPP-TETA.

Their molecular structure present all types of chemical reactive groups that may go through oxidation. For conciseness, only the CRU of the DGEBA-EDA network is presented in Fig. 8 but all three systems share similar structure. Each CRU is constituted of diethylene amine hardener moieties branched with epoxy moieties, in different proportions for each network depending on the number of reactive N−H

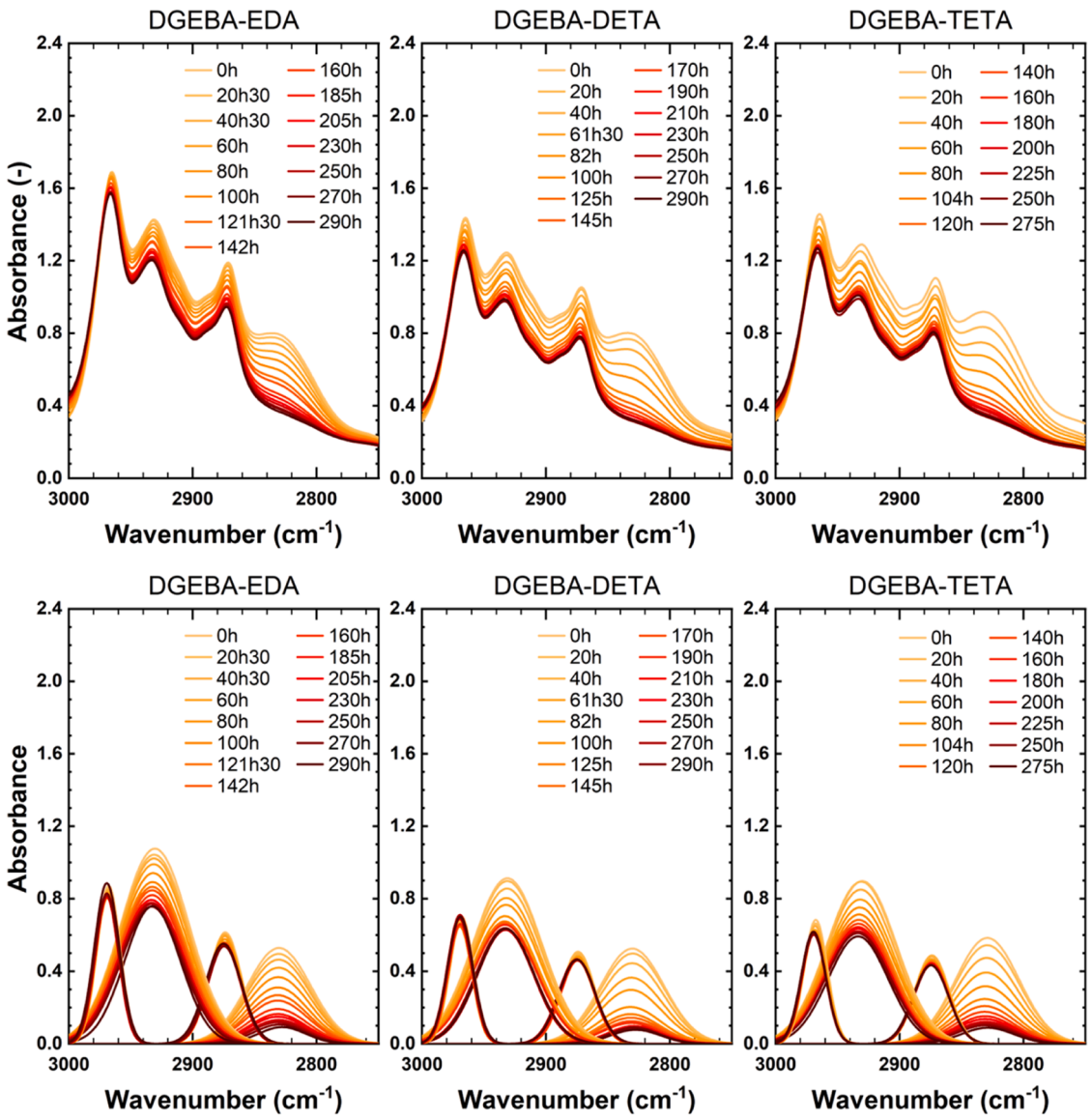

Fig. 5. (top) C-H bonds depletion during the thermal oxidation at 120°C under air. Thicknesses were normalized at 30 μm for ease of comparison – (bottom) Deconvoluted peaks of the corresponding graphs. Baseline was subtracted and the deconvolution method is described in the Suppl. Info.file.

Table 1
Assignment of FTIR peaks in the 2750–3000 cm^{-1} region[9].

Wavenumber (cm^{-1})	Allocation
3000–3100	C–H stretching
2966 (peak)	Isopropyl $–CH_3$ methyl symmetric stretching
2933 (peak)	N–C–H_2 asymmetric stretching (DGEBA)
2910 (shoulder)	N–C–H_2 asymmetric stretching (hardener)
	O–C–H_2 asymmetric stretching
2890 (shoulder)	Isopropyl $–CH_3$ methyl asymmetric stretching
2872 (peak)	N–C–H_2 symmetric stretching (DGEBA)
	O–C–H_2 symmetric stretching
2830 (peak)	N–C–H_2 symmetric stretching (hardener)

bonds of the initial aliphatic amine hardeners. The concentration of each oxidizable site is reported in Table 1.

One can observe that the three networks present a rising total concentration of amide-yielding sites (16.2 mol L^{-1} for DGEBA-EDA, 18.9 for DGEBA-DETA, and 20.6 mol L^{-1} for DGEBA-TETA), with similar concentrations of amide−yielding sites on the epoxy moiety, but very different concentrations for the hardener moiety (almost twice as much for DGEBA-TETA than for DGEBA-EDA for instance). Finally, the selectivity of oxidation is predicted by the ratio $k_{p\ hardener}$ $[>N\text{-}CH_2]_{hardener}/k_{p\ epoxy}[>N\text{-}CH_2\text{-}]_{epoxy}$which is always higher than 1 here so that the rate of degradation depends in first approach of the concentration in the utmost reactive sites ("-N-CH_2- hardener") given in Table 2 (NB: assessment of propagation rate constant will be detailed below). Oxidation is more selective at low temperature whereas oxidation kinetics appear similar when increasing the ageing temperature (see Suppl. Info. 5). A better understanding of the reactivity of those sites (expressed by the rate constant of kinetic model and their activation) remain to be determined and discussed in a future work.

Given that BDEs for the EPP-hardener molecules are representative of the polymer molecular structure, one can observe that for all three networks, O−CH_2− sites present the highest value of BDE at 413.6 kJ mol^{-1} making it the least likely to be abstracted, whether it be on a side or mid epoxy branch. −CH−OH− sites present values of 392.4 kJ mol^{-1}, making them more likely to be abstracted than O−CH_2− sites.

As for the amide-yielding groups within the structure, one can observe that "hardener" sites present BDE values between 377.9 and 380.2 kJ mol^{-1}, while "epoxy" sites present higher BDE values close between 396.0 and 397.4 kJ mol^{-1}. This significant difference of BDEs –

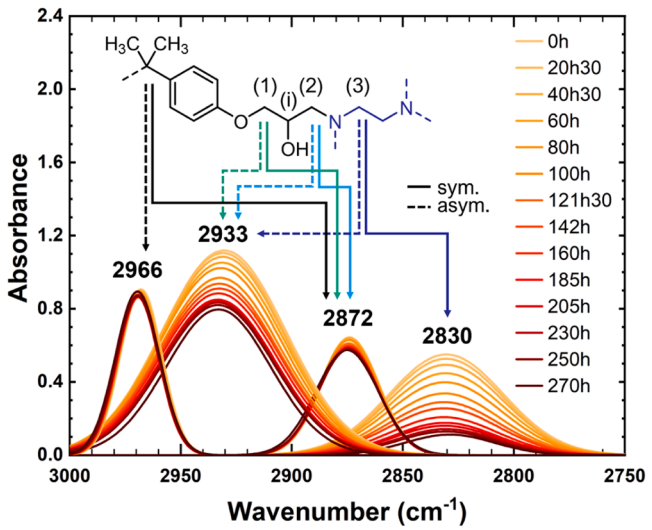

Fig. 6. Tentative assignment of the CH_2 and CH_3 groups within the molecular structure of DGEBA-EDA aged at 120 °C after deconvolution.

close to 20 kJ mol^{-1} – indicates that "hardener" sites are more prone to abstraction by peroxy radical.

Those data are in accordance with previously presented data showing that "hardener" C-H groups are consumed faster than any other sites in epoxy amine networks. Korcek et al. [23] have shown that the reaction rate, k_p, for the abstraction reaction of hydrogen atoms from unreacted sites by previously formed peroxy radicals ($POO^\circ + PH \rightarrow POOH + P^\circ$) is directly related to the BDE of the P-H bond, according to:

$$\log k_p\ (30^\circ C) = 16.2 - 0.2\ \mathrm{BDE} \quad (2)$$

$$E_P = 0.55(\mathrm{BDE} - 62.5) \quad (3)$$

Where BDE is expressed in kcal mol^{-1}.

Here, the use of those equations using for instance BDE = 380 kJ mol^{-1} for >N-CH_2 hardener, and 396 for >N-CH_2 epoxy suggests that at room temperature, the hardener methylene react almost 10 times faster than epoxy ones, but the ratio decreases at higher temperature (almost 3 at 120 °C) which seems in line with the relative decrease of absorbances at 2933 and 2830 cm^{-1} (Fig. 5)

BDE estimations and the use of Eqs. (2) and (3) also justify in part that >CH-OH are stronger than others, so that their oxidation is slow and the contribution to 1740 cm^{-1} absorbance is low (Fig. 3).

Let us now adress the effect of oxidation on the reactivity of epoxies. Some representative units of oxidized DGEBA-EDA are depicted in

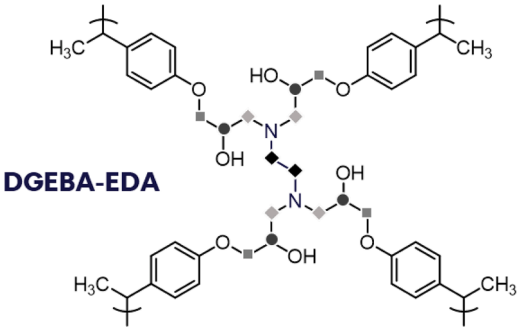

Fig. 8. Molecular structure of the constitutive repetitive unit (CRU) of DGEBA-EDA. Symbols here are further used for a better understanding of Table 2.

Table 2
Estimated [C–H] concentrations (in mol kg^{-1}) in ideal structures of the three epoxy-amine networks. N is the number of considered group, f the number of C-H reactive group and [C-H] = N.f/M_{CRU}.

System		DGEBA-EDA	DGEBA-DETA	DGEBA-TETA
CRU molar mass (g mol^{-1})		740.9	954.2	1167.4
N-CH_2 hardener	N (f=2)	2	4	6
	[C–H]	5.4	8.4	10.3
N-CH_2 epoxy	N (f=2)	4	5	6
	[C–H]	10.8	10.5	10.3
O-CH_2	N (f=2)	4	5	6
	[C–H]	10.8	10.5	10.3
CHOH	N (f=1)	4	5	6
	[C–H]	5.4	5.2	5.1

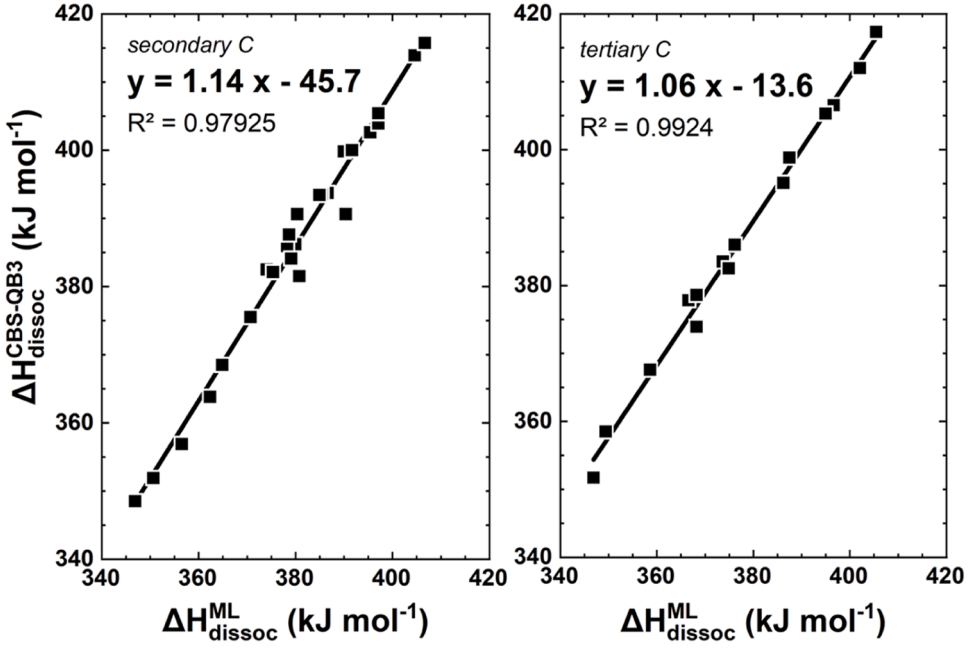

Fig. 7. C-H standard dissociation enthalpies (in kJ mol^{-1}) for C-H bonds in 40 molecules (see Supp Info.), predicted by machine learning (x-axis) and CBS-QB3 theory (y-axis).

Fig. 10, where each structure represent the possible structure resulting from radical attack of each sort of >N-CH_2-. By comparison with Fig. 9, it can mainly be seen that:

- The oxidation of a hardener methylene with no chain scission (EE=O_Nh) significantly weakens (− 8 kJ mol^{-1}) the vicinal hardener methylene.
- The oxidation of an epoxy methylene with no chain scission (EE=O_Ne) weakens (to a less extent) the closest hardener methylene (− 4 kJ mol^{-1}), while it has almost no effect (+ 1.4 kJ mol^{-1}) if there is a chain scission (EE=O*_Ne).

As hardener methylenes feature the lowest BDE, they are more likely to generate amides, and in turn, the vicinal hardener methylene becomes weaker and more susceptible to hydrogen abstraction by a peroxy radical. These results suggest that any kinetic model built at low conversion rate (when only a small part of hardener methylene has been consumed) should be completed by including the self-sensibilisation induced by the first oxidation reactions.

4.3. *On the link between CH_2 consumption and carbonyl build up*

Let us now look back at the amide build-up. Several sorts of amides (Fig. 11) can be considered:

Their population depend on the relative reactivity of CH_2 on the hardener and epoxy sides, and on the relative proportion of amide over chain scission produced, which are expected to impact the macromolecular architecture and later macroscopic properties.

To discuss on the temperature effect on the relative ratio between mechanisms leading to species depicted in Fig. 11, the depletion of hardener CH_2 was plotted against amide build-up (Fig. 12). As the molar attenuation coefficient for the FTIR signals at 2830 cm^{-1} and 1660 cm^{-1} are unknown for the systems under study, and as there is no reason that amides depicted in Fig. 11 even have the same, maxima of absorbances were plotted.

A strong correlation between the rising absorbance of amide products at 1660 cm^{-1} and the decreasing absorbance of hardener CH_2 sites is depicted. Such observations may confirm that irrespectively of ageing temperature, hardener methylene are the most affected by oxidation.

5. Conclusion

Experimental and theoretical approaches were used in this paper to study the thermal oxidation of epoxy-amine networks and its selectivity. Ageing was monitored by FTIR with an innovative discussion of the consumption of each possible oxidizable groups. It was supported by theoretical calculations with a QC corrected machine-learning approach to determine the BDE of oxidizable groups of interest in the structure. The higher sensitivity to oxidation of methylene groups located on

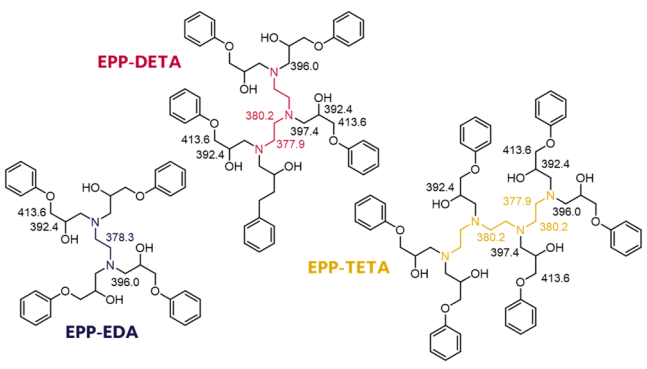

Fig. 9. BDE estimations for C−H bonds under study. BDE are expressed here in kJ mol^{-1}.

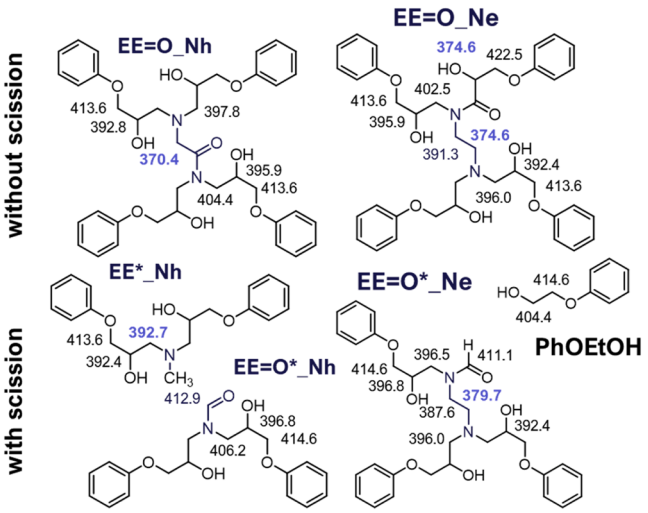

Fig. 10. Structure of oligomers representative of partially oxidized EPP-EDA and effect on selected Bond Dissociation Energies (in kJ mol^{-1}).

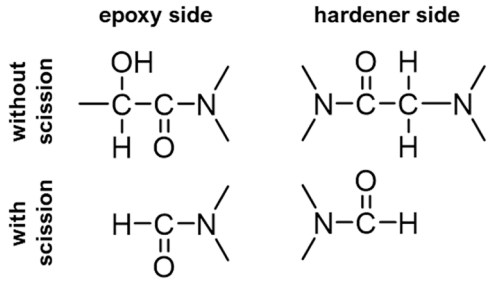

Fig. 11. Possible structures of oxidation products.

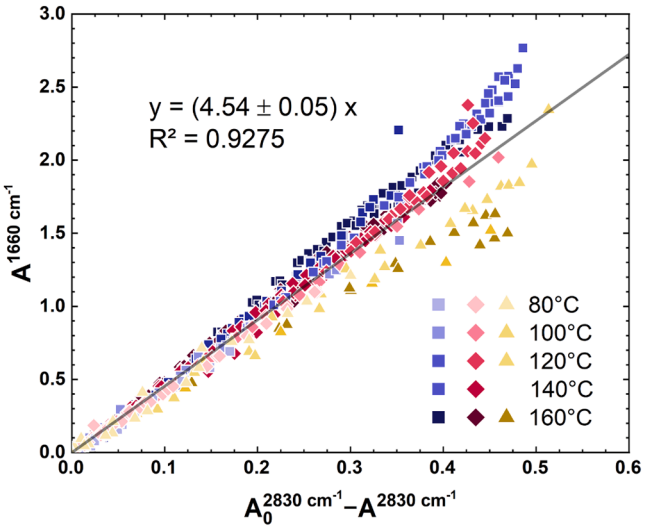

Fig. 12. Absorbance correlation between build-up of amide C=O groups and disappearance of C−H bonds. Blue squares represent DGEBA-EDA, red diamonds represent DGEBA-DETA, and yellow triangles represent DGEBA-TETA.

hardener moieties was thus explained from their lower BDE. To describe the co-oxidation of several methylene groups in α-position of nitrogen atoms simultaneously, a more complex kinetic model would have to be implemented. However, the existence of a clear correlation between methylene groups of hardener moieties consumption and amide groups formation suggests that the mechanism is representative in the

experimental conditions under investigations, and that it can therefore be extrapolated towards lower temperatures for predicting the structural changes occurring during epoxies oxidation.

CRediT authorship contribution statement

Romain Delannoy: Formal analysis, Investigation, Resources, Data curation, Writing – original draft. **Vincent Tognetti:** Conceptualization, Methodology, Software, Validation, Formal analysis, Investigation, Resources, Data curation, Writing – review & editing, Supervision. **Emmanuel Richaud:** Conceptualization, Methodology, Software, Validation, Formal analysis, Writing – original draft, Writing – review & editing, Visualization, Supervision, Project administration, Funding acquisition.

Declaration of Competing Interest

We hereby confirm that we have no conflict of interest with the paper "Experimental and theoretical insights on the thermal oxidation of epoxy-amine networks" submitted to Polymer Degradation and Stability.

Data Availability

Data will be made available on request.

Acknowledgments

The Agence Nationale de la Recherche is gratefully acknowledged for funding the project ANR DUREVE (18-CE-0028, 2019-2022).

References

[1] C.A. May, Y. Tanaka, C. May, T. Tanaka, Epoxy resins. Chemistry and Technology, Marcel Dekker, Inc., 1973 (Eds.).
[2] E. Morel, V. Bellenger, J. Verdu, Structure-water absorption relationships for amine-cured epoxy resins, Polymer 26 (11) (1985) 1719–1724, https://doi.org/10.1016/0032-3861(85)90292-7 *(Guildf)*.
[3] D.N. Dang, S. Cohendoz, S. Mallarino, X. Feaugas, S. Touzain, Effects of curing program on mechanical behavior and water absorption of DGEBA/TETa epoxy network, J. Appl. Polym. Sci. 129 (5) (2013) 2451–2463, https://doi.org/10.1002/app.38843.
[4] G.Z. Xiao, M.E.R. Shanahan, Water absorption and desorption in an epoxy resin with degradation, J. Polym. Sci. Part B Polym. Phys. 35 (16) (1997) 2659–2670, https://doi.org/10.1002/(SICI)1099-0488(19971130)35:16<2659::AID-POLB9>3.0.CO;2-K.
[5] S. Montserrat, P. Cortés, A. Pappin, K. Quah, J. Hutchinson, Structural relaxation in fully cured epoxy resins, J. Non Cryst. Solids 172 (1994) 1017–1022, https://doi.org/10.1016/0022-3093(94)90615-7. *–174.*
[6] F. Djouani, Y. Zahra, B. Fayolle, M. Kuntz, J. Verdu, Degradation of epoxy coatings under gamma irradiation, Radiat. Phys. Chem. 82 (2013) 54–62, https://doi.org/10.1016/j.radphyschem.2012.09.008.
[7] Y. Zahra, F. Djouani, B. Fayolle, M. Kuntz, J. Verdu, Thermo-oxidative aging of epoxy coating systems, Prog. Org. Coat. (2014), https://doi.org/10.1016/j.porgcoat.2013.10.011.
[8] N. Longiéras, M. Sebban, P. Palmas, A. Rivaton, J.L. Gardette, Degradation of epoxy resins under high energy electron beam irradiation: radio-oxidation, Polym. Degrad. Stab. 92 (12) (2007) 2190–2197, https://doi.org/10.1016/j.polymdegradstab.2007.01.035.
[9] M.C. Celina, A.R. Dayile, A. Quintana, A perspective on the inherent oxidation sensitivity of epoxy materials, Polymer 54 (13) (2013) 3290–3296, https://doi.org/10.1016/j.polymer.2013.04.042 *(Guildf)*.
[10] D. Bertin, M. Leblanc, S.R.A. Marque, D. Siri, Polypropylene degradation: theoretical and experimental investigations, Polym. Degrad. Stab. 95 (5) (2010) 782–791, https://doi.org/10.1016/j.polymdegradstab.2010.02.006.
[11] X. Colin, L. Audouin, J. Verdu, Kinetic modelling of the thermal oxidation of polyisoprene elastomers. part 1: unvulcanized unstabilized polyisoprene, Polym. Degrad. Stab. 92 (5) (2007) 886–897, https://doi.org/10.1016/j.polymdegradstab.2007.01.017.
[12] P.Y. Le Gac, G. Roux, J. Verdu, P. Davies, B Fayolle, Oxidation of unvulcanized, unstabilized polychloroprene: a kinetic study, Polym. Degrad. Stab. 109 (2014) 175–183, https://doi.org/10.1016/j.polymdegradstab.2014.06.019.
[13] J. Delozanne, N. Desgardin, N. Cuvillier, E. Richaud, Thermal oxidation of aromatic epoxy-diamine networks, Polym. Degrad. Stab. (2019), https://doi.org/10.1016/j.polymdegradstab.2019.05.030.
[14] M.C. Celina, E. Linde, E. Martinez, Carbonyl identification and quantification uncertainties for oxidative polymer degradation, Polym. Degrad. Stab. 188 (2021), 109550, https://doi.org/10.1016/j.polymdegradstab.2021.109550.
[15] V. Bellenger, J. Verdu, E. Morel, Effect of structure on glass transition temperature of amine crosslinked epoxies, J. Polym. Sci. Part B Polym. Phys. 25 (6) (1987) 1219–1234, https://doi.org/10.1002/polb.1987.090250604.
[16] M.G. González, J.C. Cabanelas, J. Baselga, Applications of FTIR on epoxy resins - identification, monitoring the curing process, phase separation and water uptake. Infrared Spectroscopy - Materials Science, Engineering and Technology, InTech, 2012, https://doi.org/10.5772/36323.
[17] B. Mailhot, S. Morlat-Thérias, P.O. Bussière, J.L. Gardette, Study of the degradation of an epoxy/amine resin, 2 kinetics and depth-profiles, Macromol. Chem. Phys. 206 (5) (2005) 585–591, https://doi.org/10.1002/macp.200400394.
[18] N.H. Giron, M.C. Celina, High temperature polymer degradation: rapid IR flow-through method for volatile quantification, Polym. Degrad. Stab. 145 (2017) 93–101, https://doi.org/10.1016/j.polymdegradstab.2017.05.013.
[19] B.H. Stuart, Infrared Spectroscopy: Fundamentals and Applications, Wiley, 2005, https://doi.org/10.1002/0470011149.
[20] X. Colin, L. Audouin, J. Verdu, Determination of thermal oxidation rate constants by an inverse method. application to polyethylene, Polym. Degrad. Stab. 86 (2) (2004) 309–321, https://doi.org/10.1016/j.polymdegradstab.2004.04.022.
[21] J.A. Montgomery, M.J. Frisch, J.W. Ochterski, G.A. Petersson, A complete basis set model chemistry. VI. use of density functional geometries and frequencies, J. Chem. Phys. 110 (6) (1999) 2822–2827, https://doi.org/10.1063/1.477924.
[22] M.J. Frisch, G.W. Trucks, H.B. Schlegel, G.E. Scuseria, M.A. Robb, J.R. Cheeseman, G. Scalmani, V. Barone, B. Mennucci, G.A. Petersson, H. Nakatsuji, M. Caricato, X. Li, H.P. Hratchian, A.F. Izmaylov, J. Bloino, G. Zheng, J.L. Sonnenberg, M. Hada, M. Ehara, K. Toyota, R. Fukuda, J. Hasegawa, M. Ishida, T. Nakajima, Y. Honda, O. Kitao, H. Nakai, T. Vreven, J.A. Montgomery, Jr, J.E. Peralta, F. Ogliaro, M. Bearpark, J.J. Heyd, E. Brothers, K.N. Kudin, V.N. Staroverov, T. Keith, R. Kobayashi, J. Normand, K. Raghavachari, A. Rendell, J.C. Burant, S.S. Iyengar, J. Tomasi, M. Cossi, N. Rega, J.M. Millam, M. Klene, J.E. Knox, J.B. Cross, V. Bakken, C. Adamo, J. Jaramillo, R. Gomperts, R.E. Stratmann, O. Yazyev, A. J. Austin, R. Cammi, C. Pomelli, J.W. Ochterski, R.L. Martin, K. Morokuma, V. G. Zakrzewski, G.A. Voth, P. Salvador, J.J. Dannenberg, S. Dapprich, A.D. Daniels, O. Farkas, J.B. Foresman, J.V. Ortiz, J. Cioslowski, D.J. Fox, Gaussian 09, Revision D.01, Gaussian, Inc., Wallingford CT, 2013.
[23] S. Korcek, J.H.B. Chenier, J.A. Howard, K.U. Ingold, Absolute rate constants for hydrocarbon autoxidation. XXI. activation energies for propagation and the correlation of propagation rate constants with carbon–hydrogen bond strengths, Can. J. Chem. 50 (14) (1972) 2285–2297, https://doi.org/10.1139/v72-365.